




ORIGINAL ARTICLE

# A novel intelligent chromo capsule endoscope for the diagnosis of neoplastic lesions in the gastrointestinal tract

Huiying Shi <sup>1,†</sup>, Suyu Pang<sup>1,†</sup>, Fanhua Ming<sup>2</sup>, Tianyi Yangdai<sup>2</sup>, Shuxin Tian<sup>1,3</sup> and Rong Lin<sup>1,\*</sup>

<sup>1</sup>Department of Gastroenterology, Union Hospital, Tongji Medical College, Huazhong University of Science and Technology, Wuhan, Hubei, P. R. China; <sup>2</sup>Ankon Technologies Co., Ltd, Wuhan, Hubei, P. R. China; <sup>3</sup>Department of Gastroenterology, The First Affiliated Hospital of Medical College, Shihezi University, Shihezi, Xinjiang, P. R. China

\*Corresponding author. Department of Gastroenterology, Union Hospital, Tongji Medical College, Huazhong University of Science and Technology, 1277 Jiefang Avenue, Wuhan 430022, P. R. China. Tel: +86-27-85726085; Email: linrong@hust.edu.cn

<sup>†</sup>These authors contributed equally to this paper.

## Abstract

**Background:** Chromoendoscopy has not been fully integrated into capsule endoscopy. This study aimed to develop and validate a novel intelligent chromo capsule endoscope (ICCE).

**Methods:** The ICCE has two modes: a white-light imaging (WLI) mode and an intelligent chromo imaging (ICI) mode. The performance of the ICCE in observing colors, animal tissues, and early gastrointestinal (GI) neoplastic lesions in humans was evaluated. Images captured by the ICCE were analysed using variance of Laplacian (VoL) values or image contrast evaluation.

**Results:** For color observation, conventional narrow-band imaging endoscopes and the ICI mode of the ICCE have similar spectral distributions. Compared with the WLI mode, the ICI mode had significantly higher VoL values for animal tissues ( $2.154 \pm 1.044$  vs  $3.800 \pm 1.491$ ,  $P = 0.003$ ), gastric precancerous lesions and early gastric cancers ( $2.242 \pm 0.162$  vs  $6.642 \pm 0.919$ ,  $P < 0.001$ ), and colon tumors ( $3.896 \pm 1.430$  vs  $11.882 \pm 7.663$ ,  $P < 0.001$ ), and significantly higher contrast for differentiating tumor and non-tumor areas ( $0.069 \pm 0.046$  vs  $0.144 \pm 0.076$ ,  $P = 0.005$ ). More importantly, the sensitivity, specificity, and accuracy of the ICI mode for early GI tumors were 95.83%, 91.67%, and 94.64%, respectively, which were significantly higher than the values of the WLI mode (78.33% [ $P < 0.001$ ], 77.08% [ $P = 0.01$ ], and 77.98% [ $P < 0.001$ ], respectively).

**Conclusions:** We successfully integrated ICI into the capsule endoscope. The ICCE is an innovative and useful tool for differential diagnosis based on contrast-enhanced images and thus has great potential as a superior diagnostic tool for early GI tumor detection.

**Key words:** capsule endoscopy; chromoendoscopy; intelligent chromo capsule endoscope; white-light imaging; intelligent chromo imaging

Submitted: 12 November 2022; Revised: 15 March 2023; Accepted: 16 March 2023

© The Author(s) 2023. Published by Oxford University Press and Sixth Affiliated Hospital of Sun Yat-sen University

This is an Open Access article distributed under the terms of the Creative Commons Attribution-NonCommercial License (<https://creativecommons.org/licenses/by-nc/4.0/>), which permits non-commercial re-use, distribution, and reproduction in any medium, provided the original work is properly cited.

For commercial re-use, please contact [journals.permissions@oup.com](mailto:journals.permissions@oup.com)

## Introduction

Gastrointestinal (GI) cancers, including gastric cancer, colorectal cancer, and esophageal cancer, are common malignant tumors and the leading cause of cancer deaths worldwide [1]. Digestive endoscopy is an important tool for the early diagnosis and treatment of GI tumors, which is critical for reducing morbidity and mortality [2–4].

Electronic chromoendoscopy technologies such as digital and optical chromoendoscopy provide image enhancement and may improve the diagnosis of mucosal lesions [5]. Digital chromoendoscopy includes Fuji intelligent color enhancement and i-SCAN, and optical chromoendoscopy includes narrow-band imaging (NBI), blue-light imaging, and linked-color imaging. In NBI, a special filter after the light source restricts the incident light to two narrow bands with wavelengths of 415 nm (blue) and 540 nm (green) [6]. The blue and green bands are absorbed by hemoglobin in blood vessels, which can be reflected by the mucosal surface, thereby enhancing the tissue microvasculature. Thus, NBI provides unique images that emphasize the surface, mucosal, and submucosal vasculature of lesions in the GI tract [7]. NBI is useful for differentiating neoplasms from non-neoplasms and for predicting histopathological diagnosis for mucosal lesions in the GI tract [8] and has better diagnostic performance than conventional white-light imaging (WLI) [9].

Currently, NBI technology is installed on conventional endoscopes and combined with magnification endoscopy. However, conventional endoscopy uses a long, flexible endoscope, which is invasive and may prevent its use in patients with severe underlying disease and poor tolerance [10]. These issues can be addressed by capsule endoscopy (CE). Magnetically controlled CE is a non-invasive endoscopy technique with better tolerability than conventional endoscopy [11, 12], although it cannot be used in patients with obstruction due to the risk of capsule retention. The control accuracy of magnetically controlled CE is slightly lower than that of a conventional endoscope, and the biopsy and spraying functions of CE are still under development [13]. Studies have shown that the diagnostic accuracy of magnetically controlled CE is comparable to that of conventional gastroscopy [14, 15]. In addition, CE minimizes aerosol generation and is safer than conventional endoscopy, particularly in the current era of the coronavirus disease 2019 (COVID-19) pandemic [16].

However, chromo imaging is not available for CE in clinical practice. Therefore, this study developed a new type of CE that combines the noninvasiveness and flexibility of CE with image-enhancing endoscopy technology to observe the microscopic structure and microvessels of the mucosal surface of the GI tract and improve the diagnostic performance of CE for GI tumors.

## Methods

### Intelligent chromo capsule endoscope and study design

An intelligent chromo capsule endoscope (ICCE) was developed in this study, and its performance in observing colors, animal tissues, and early GI neoplastic lesions was evaluated.

The overall design of the ICCE is illustrated in Figure 1A. The ICCE has two observation modes: WLI (Figure 1B) and intelligent chromo imaging (ICI) (Figure 1C). The ICCE (26 mm × 11.6 mm) is composed of four main parts: an imaging module consisting of a camera, 10 light-emitting diodes (LEDs), and a vertical-cavity surface-emitting laser; batteries; a microcontroller unit; and a

wireless transmission module. The light source has three types of LEDs: four white-color LEDs, four blue-color LEDs with a wavelength of 415 nm, and two green-color LEDs with a wavelength of 540 nm (Figure 1D). The detailed spectral information is shown in Table 1. In both modes, the image resolution is 480 × 480 and the maximum frame rate is 6 frames/s.

The WLI mode is the traditional imaging mode and is suitable for observing the mucosal surface of the digestive tract. Images are captured when the white-color LEDs are on. The whole WLI system is identical to the current CE with proven effectiveness [17, 18].

The ICI mode combines blue-color and green-color LEDs. Blue light is strongly absorbed by hemoglobin in the shallow depth of the mucosa that is permeated with surface blood vessels, and green light is transmitted to the middle depth of the mucosa and the middle-depth blood vessels [19]. Therefore, the ICI mode is able to enhance the visualization of blood vessels. The relative intensity of these LEDs can be adjusted by adjusting the voltage through pulse width modulation to achieve the best observation effect.

The study was approved by the Ethics Committee of Tongji Medical College, Huazhong University of Science and Technology (IORG No. IORG0003571), was registered in the Chinese Clinical Trial Registry (registration No. ChiCTR2200058461), and was performed in accordance with the Declaration of Helsinki. The animal study was approved by the Animal Experimentation Ethics Committee of Huazhong University of Science and Technology.

### Observations of colors

To evaluate the imaging effects of the ICCE on different colors, we used conventional NBI magnifying endoscopy and the ICCE to observe a circular 18-color palette and collected images. As the field of view and depth of field of the capsule are limited, to ensure a consistent imaging effect of each color, six gray cards were removed from the 24-color standard color card to construct the circular 18-color palette. Detailed information about the 24-color standard color card and the 18-color palette is provided in Supplementary Figure 1. The numbers 1–18 on the color palette in Figure 2A correspond to the numbers 1–18 in Supplementary Figure 1B. The red–green–blue images taken by the conventional NBI endoscope and ICCE were converted to International Commission on Illumination (CIE)  $L^*a^*b^*$  color values using the D50 reference white. The  $L^*a^*b^*$  color model consists of three elements: brightness ( $L^*$ ) and two independent color channels ( $a^*$  for green-to-red and  $b^*$  for blue-to-yellow). The orthogonality of  $L^*$ ,  $a^*$ , and  $b^*$  enables the 3D representation of colors and ultimately provides three sensing factors in our sensing platform [20]. As the brightness ( $L^*$ ) could be influenced by exposure conditions, only the  $a^*$  and  $b^*$  values of the  $L^*a^*b^*$  images were analysed. The sampling areas on the color blocks were marked by white circles with green number marks. Each sampling area consisted of  $5 \times 5$  pixels and the average value of the pixels was calculated.

### Animal experiments

Male Sprague–Dawley rats weighing ~230 g were purchased from SPF (Beijing) Biotechnology Co., Ltd. Three rats were fasted the night before the experiment. The rats were intraperitoneally anesthetized with 3% chloral hydrate and their stomachs were observed. The WLI and ICI modes of the ICCE were used to observe the same regions of the stomachs in the dark and images were collected.

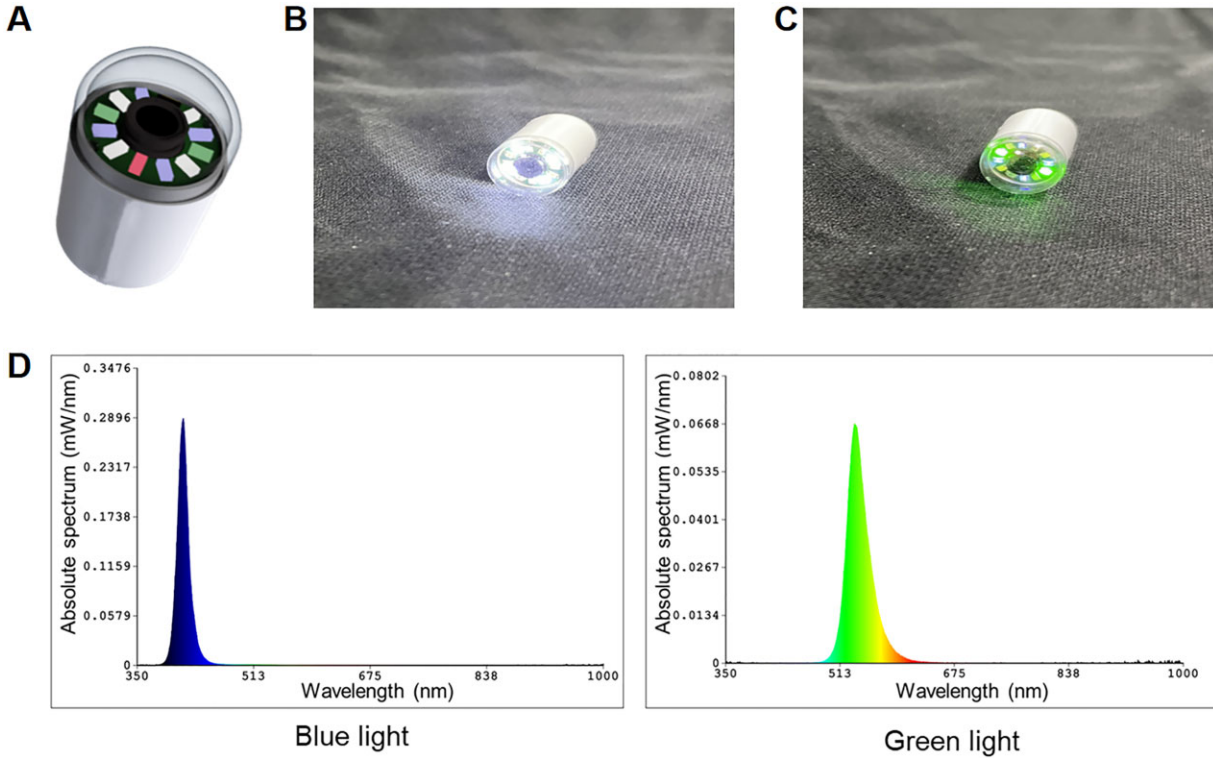


**Figure 1.** The overall design of the ICCE. (A) The ICCE (the red cube represents the vertical-cavity surface-emitting laser); (B) the image of the ICCE model in the WLI mode; (C) the image of the ICCE in the ICI mode; (D) the spectra of the blue and green light. WLI, white-light imaging; ICI, intelligent chromo imaging; ICCE, intelligent chromo capsule endoscope.

**Table 1.** Spectral information of the blue and green light

Type	Central wavelength (nm)	Peak wavelength (nm)	Full width at half maxima (nm)
Blue light	435.3	413.7	16.7
Green light	544.1	532.9	32.2

### Comparison of the ICI and WLI modes in differentiating tumor lesions and non-tumor lesions

The diagnostic performance of the ICCE was tested on 20 early GI tumor lesions and 8 non-tumor lesions. All lesions were observed in both WLI and ICI modes, and images were captured. After imaging, the specimens were immersed in formaldehyde and routine histopathological examinations were conducted. The histopathological diagnosis was considered the gold standard. Gastroenterologists (six experienced doctors and six inexperienced doctors) reviewed the images and made diagnoses separately in WLI mode and ICI mode. All participating gastroenterologists were blinded to the histopathological diagnoses. The diagnostic performance of the WLI and ICI modes of the ICCE was evaluated by comparison with the histopathological diagnosis.

### Image sharpness evaluation

The variance of Laplacian (VoL), a traditional image sharpness evaluation operator [21, 22], was used to analyse the images taken by the ICCE in the WLI and ICI modes. Compared with other traditional image sharpness operators, Laplacian-based

operators have better overall performance under normal imaging conditions. The VoL utilizes the variance of the image Laplacian, which is defined as follows:

$$\phi = \sum (I_L(x, y) - \bar{I}_L)^2$$

where  $\bar{I}_L$  is the mean value of the image Laplacian  $I_L$ . Higher  $\phi$  values indicate sharper images.

### Image contrast evaluation

To quantify the image contrast between lesion and non-lesion areas, the following formula was used [19]:

$$\text{Contrast} = \frac{|Y_N - Y_L|}{Y_N}$$

Here,  $Y = 0.299R + 0.587G + 0.114B$  is the brightness of a pixel in the red-green-blue image, where  $R$ ,  $G$ , and  $B$  represent the pixel values of the R, G, and B channels, respectively.  $Y_N$  and  $Y_L$  represent the average brightness of the non-lesion and lesion areas, respectively.

### Statistical analysis

GraphPad Prism v6.0c (GraphPad Software, San Diego, CA, USA) or MATLAB 2015a (The MathWorks, Inc.) was used for the statistical analysis of the experimental data, which are expressed as the mean  $\pm$  standard deviation of at least three independent experiments. The t-test was used to compare the VoL and contrast values between the WLI and ICI modes. A value of  $P < 0.05$  was considered statistically significant.

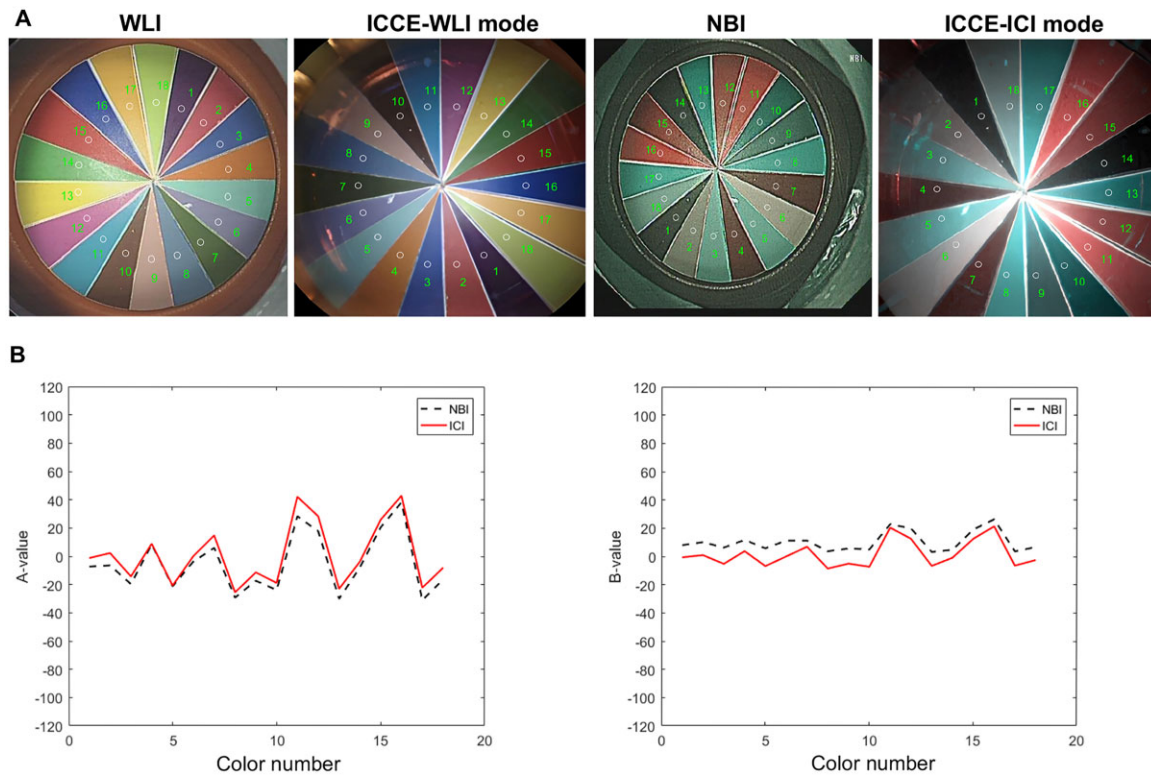


**Figure 2.** Imaging comparison of the ICCE and conventional NBI endoscopy in color observation. (A) Representative images of the 18-color palette acquired in the WLI and NBI modes of the Olympus endoscope (left panel) and the WLI and ICI modes of the ICCE (right panel); (B)  $a^*$  and  $b^*$  values of the  $L^*a^*b^*$  images of the 18-color palette acquired in the NBI mode of the Olympus endoscope and the ICI mode of the ICCE. WLI, white-light imaging; ICCE, intelligent chromo capsule endoscope; NBI, narrow-band imaging; ICI, intelligent chromo imaging.

## Results

### The ICCE and conventional NBI endoscopy have similar spectral distributions in color imaging

To evaluate color imaging by the ICI mode of the ICCE, both the conventional NBI endoscope and the ICCE were used to observe an 18-color palette (Figure 2A). As shown in Figure 2B, the colors of each color block were similar between the ICI mode and conventional NBI, which shows that the two systems have similar spectral distributions.

### Imaging of rat gastric mucosa by the ICCE

We used the ICCE to observe the blood vessels on the rat gastric serosal surface (Figure 3A and B). The ICI mode of the ICCE clearly imaged the blood vessels on the gastric serosal surface, including thick blood vessels and fine blood vessels (Figure 3B). The VoL values were higher in the ICI mode than those in the WLI mode ( $3.800 \pm 1.491$  vs  $2.154 \pm 1.044$ ,  $P = 0.003$ , Figure 3C), indicating that the ICI mode had an image enhancement effect and provided clearer images, which may improve the diagnosis of mucosal lesions in the GI tract.

### The ICI mode is superior to the WLI mode in observing early neoplastic lesions in the GI tract

The ability of the WLI and ICI modes to diagnose gastric precancerous lesions and early gastric cancer lesions was evaluated by observing seven cases of high-grade intraepithelial neoplasia and intramucosal carcinoma, and one case of low-grade intraepithelial neoplasia. The ICI mode clearly imaged irregular

mucosal microsurface and microvasculature of a gastric precancerous lesion (Figure 4A–C) and more representative images of gastric precancerous lesions and early gastric cancer lesions are shown in Supplementary Figure 2. Compared with the WLI mode, the ICI mode had higher VoL values ( $2.242 \pm 0.162$  vs  $6.642 \pm 0.919$ ,  $P < 0.0001$ ) (Figure 4D).

The ability of the WLI and ICI modes to diagnose early colonic tumors was evaluated by observing eight cases of tubulovillous adenomas and one case of neuroendocrine tumor. The ICI mode clearly displayed the vessel and surface patterns of the colonic tumor (Figure 5A–C) and more representative images of colonic tumors are shown in Supplementary Figure 3. Similarly, the ICI mode showed superior VoL values than the WLI mode ( $11.882 \pm 7.663$  vs  $3.896 \pm 1.430$ ,  $P < 0.0001$ ) (Figure 5D).

### Discrimination contrast of the ICI mode for non-tumor lesion and tumor lesion areas

The ICI mode of the ICCE clearly distinguished tumor areas from non-tumor areas (Figure 6A–D). The ICI mode had a higher discrimination contrast between tumor and non-tumor areas than the WLI mode ( $0.144 \pm 0.076$  vs  $0.069 \pm 0.046$ ,  $P = 0.005$ ) (Figure 6E and Table 2). The high discrimination contrast between tumor and non-tumor areas under the ICI mode may be helpful for the detection of GI tumors.

### Diagnostic accuracy of the WLI and ICI modes on early GI tumor specimens

To assess diagnostic performance, images of 20 early GI tumor lesions and 8 non-tumor lesions acquired in the WLI and ICI



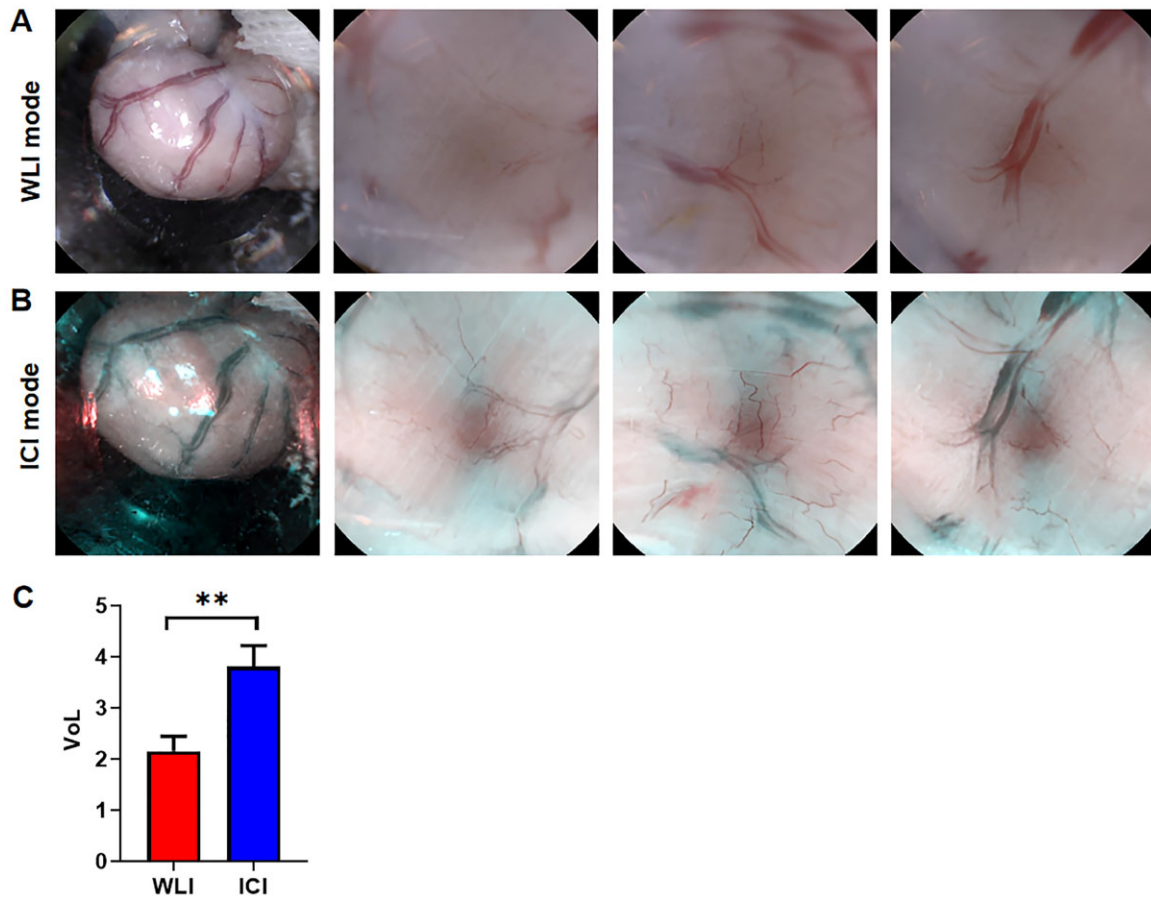


**Figure 3.** Comparison of WLI and ICI modes in observation of stomach in rats. (A) Representative images of rat stomach acquired in the WLI mode of the ICCE; (B) representative images of rat stomach acquired in the ICI mode of the ICCE; (C) the VoL values of rat stomach images were significantly higher in the ICI mode than those in the WLI mode. WLI, white-light imaging; ICI, intelligent chromo imaging; ICCE, intelligent chromo capsule endoscope; VoL, Variance of Laplacian. \*\* $P < 0.01$ .

modes were reviewed and diagnosed by endoscopists. The representative images of non-tumor lesions acquired under the WLI and ICI modes are shown in [Supplementary Figure 4](#). The 20 early GI lesions included eight cases of tubulovillous adenoma, seven cases of high-grade intraepithelial neoplasia and intramucosal carcinoma, one case of low-grade intraepithelial neoplasia, three cases of esophageal squamous cell carcinoma, and one case of neuroendocrine tumor. For experienced endoscopists, the ICI mode had significantly higher sensitivity [95.83% [95% confidence interval {CI}, 90.00%–100%] vs 78.33% [95% CI, 65.00%–85.00%],  $P = 0.0005$ ], specificity (91.67% [95% CI, 87.50%–100%] vs 77.08% [95% CI, 62.50%–87.50%],  $P = 0.01$ ) and accuracy (94.64% [95% CI, 89.29%–100%] vs 77.98% [95% CI, 67.86%–85.71%],  $P = 0.0002$ ) than the WLI mode. For inexperienced gastroenterologists, the accuracy of the ICI was also significantly higher than that of the WLI mode (87.50% [95% CI, 78.57%–96.43%] vs 72.62% [95% CI, 64.29%–78.57%],  $P < 0.01$ ).

## Discussion

In this study, we developed a novel intelligent chromo CE and validated its performance in observing colors, animal tissues, and early GI neoplastic lesions in humans. Several highlights should be emphasized in our study. First, to our knowledge, this is the first study to integrate chromo imaging functions into CE. Second, we found that the ICCE has a good imaging in color and

animal tissue. More importantly, the ICI mode is superior to the WLI mode in observing early GI neoplastic lesions.

Early detection and treatment of GI cancer is crucial and endoscopic screening can reduce GI cancer mortality in high-risk countries [23]. Although conventional endoscopy is the current gold standard for clinical diagnosis, due to limited endoscopy resources, poor patient acceptance, adverse GI events, and the risk of anesthesia, early cancer screening in large populations has not been achieved.

CE can be used to examine the esophagus, stomach, small intestine, and large intestine, and the advent of magnetically controlled capsule endoscopes allows endoscopists to make detailed observations of the GI mucosal surface [24–26]. By applying an external magnetic field, the position and direction of the capsule can be actively controlled in magnetically controlled CE systems, thereby allowing a comprehensive observation of the gastric mucosa and upper GI tract [18, 27]. Compared with conventional gastroscopy, magnetically controlled capsule gastroscopy has similar sensitivity, specificity, and overall accuracy in the diagnosis of gastric diseases and is better tolerated by patients [28, 29]. Similarly, colon CE has proved to be a safe and effective tool for the detection of colorectal cancer, and the diagnostic accuracy of colon CE for colon cancer and polyp detection is equivalent to that of colonoscopy [30].

Electronic chromoendoscopy has high sensitivity for detecting early GI neoplastic lesions by observing mucosal microstructure and microvessels [31, 32]. Compared with WLI, NBI

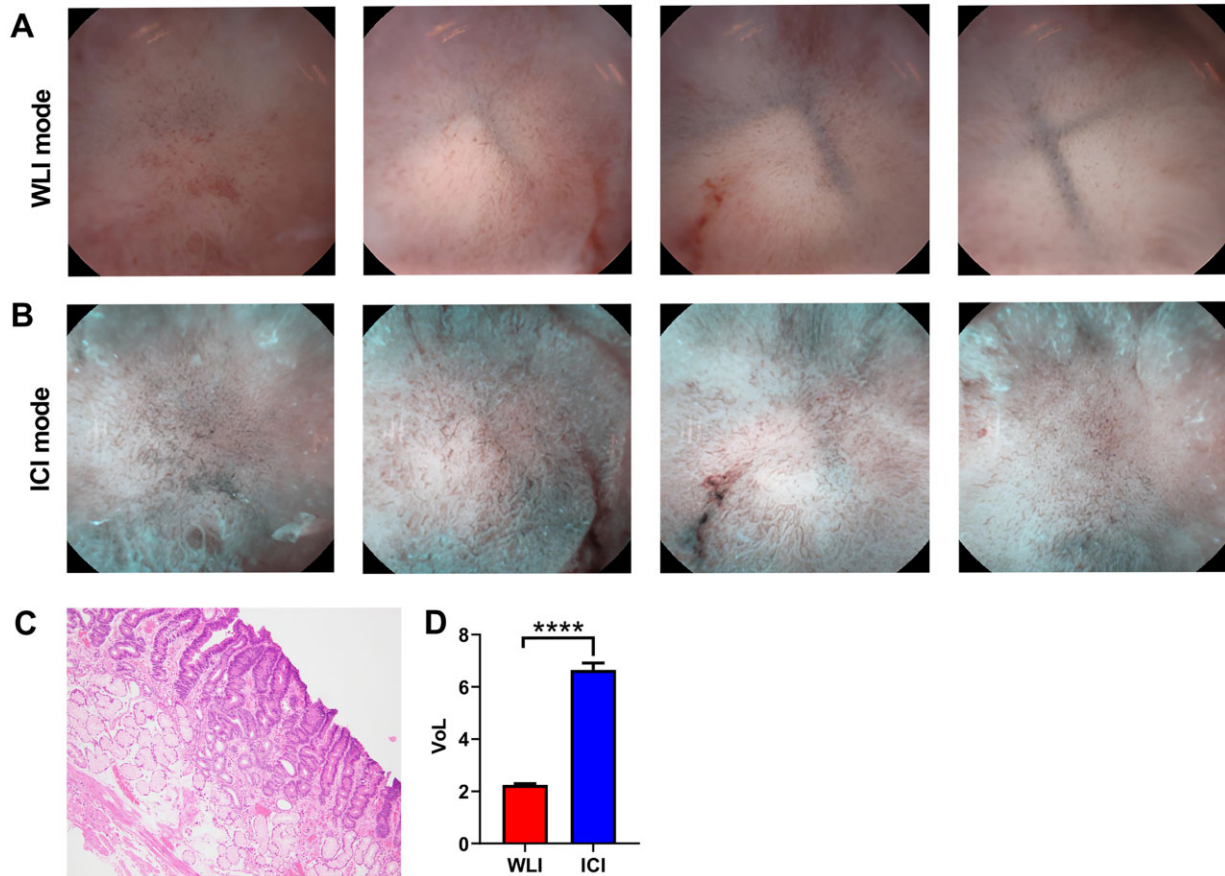


**Figure 4.** Imaging comparison of WLI and ICI modes in observation of early GI neoplastic lesions. (A) and (B) Representative images of different regions of a gastric precancerous lesion acquired in the WLI mode (A) and ICI mode (B) of the ICCE; (C) histopathology showed low-grade intraepithelial neoplasia; (D) the Vol values of gastric precancerous lesion and early gastric cancers (eight lesions) images were significantly higher in the ICI mode than in the WLI mode. WLI, white-light imaging; ICI, intelligent chromo imaging; ICCE, intelligent chromo capsule endoscope; Vol, Variance of Laplacian. \*\*\*\* $P < 0.0001$ .

significantly improves the rate of detection of GI cancers [33, 34]. However, the observation of the GI mucosa by CE has been mainly limited to WLI. Integrating electronic chromoendoscopy into CE may facilitate the diagnosis of GI diseases, especially neoplastic diseases. Therefore, in this study, we developed ICCE and evaluated its ability to image colors, animal tissues, and human specimens *in vitro*. The ICI mode of the ICCE and conventional NBI had similar observation performance on an 18-color palette. The ICI mode could clearly image mucosal surface blood vessels in both animal models and human GI tumors. In addition, the ICI mode provided clear images of abnormal blood vessels in neoplastic lesions of the GI mucosa. Compared with the WLI mode, the ICI mode of the ICCE provided higher discrimination contrast between tumor and non-tumor areas, which can facilitate their differentiation. Most importantly, the overall accuracy of the ICI mode for the diagnosis of early GI neoplastic lesions was significantly higher than that of the WLI mode. Therefore, we believe that the ICI mode is a good auxiliary diagnostic function of CE.

Although several studies over the past decade have focused on the development of NBI capsule endoscopes, none is available on the market. In 2010, Dung et al. [35] developed a capsule endoscope that incorporates an NBI chip and tested it on the backside mucosa of human tongue and porcine small intestine. They found that the NBI capsule endoscope significantly improved image quality but did not test it on human specimens or evaluate its ability to detect GI tumors. In 2018, Yen et al. [36]

proposed an optical design with NBI for a capsule endoscope and focused on the design and optimization of optics in the capsule system. By contrast, we not only developed an ICCE with image enhancement but also validated its application in animal and human GI tumor diagnosis, bringing this technology a step closer to clinical application.

This study has several limitations. First, the diagnostic performance of the ICI mode was only validated by observing lesions at close distances. The ability of the WLI and ICI modes to detect suspicious lesions at “screening” distances will be compared in a future study. Second, similarly to common CE, the ICCE requires magnetic control for complete imaging of the GI mucosa. The magnetic control design and data need to be further improved. Third, well-designed prospective studies are needed to confirm the imaging effects.

## Conclusions

We successfully integrated ICI into a capsule endoscope. The ICCE adds the ICI mode to all of the functions of a traditional white-light capsule. The effectiveness of the ICI mode of the ICCE surpassed that of the WLI used in clinical practice. The ICCE enabled excellent imaging of color and animal and human specimens. Furthermore, the WLI and ICI modes can be switched at will through wireless control to meet the needs of diagnosis, which has the potential to expand the clinical application of CE as a diagnostic tool for the GI tract.

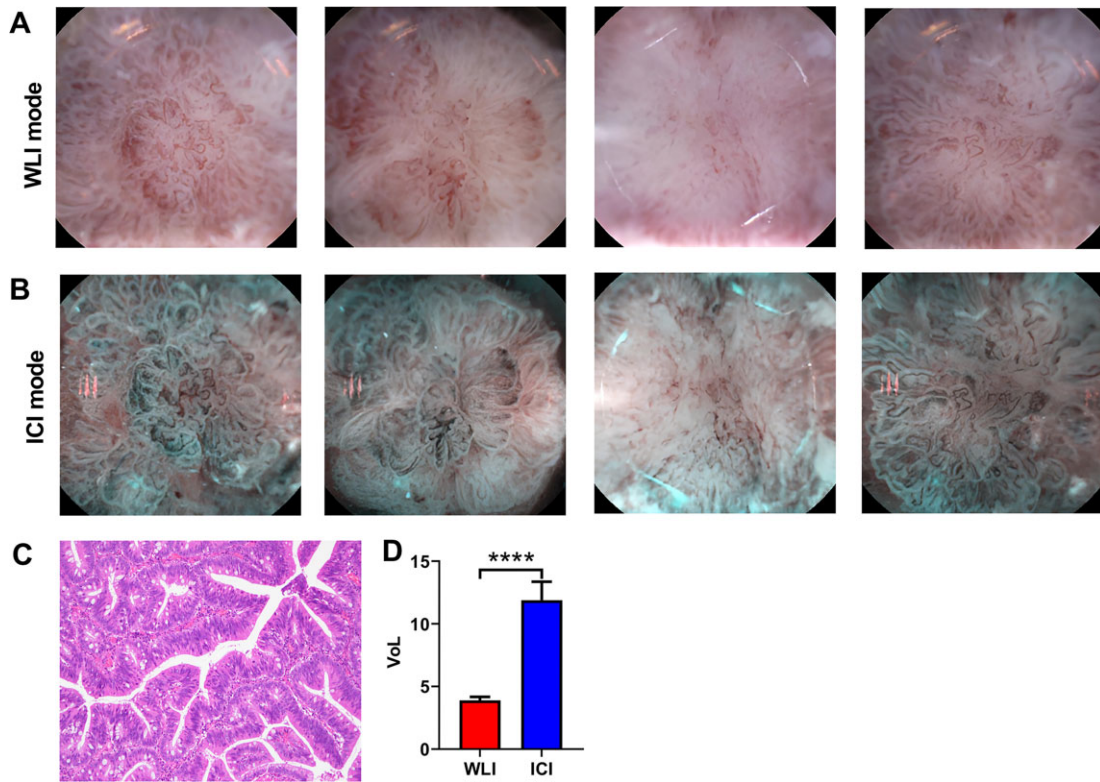


**Figure 5.** Imaging comparison of WLI and ICI modes in observation of the early colonic tumors. (A) and (B) Representative images of different regions of a colonic tumor lesion acquired in the WLI mode (A) and ICI mode (B) of the ICCE; (C) histopathology showed tubulovillous adenoma; (D) the VoL values of colonic tumor (nine lesions) images were significantly higher in the ICI mode than in the WLI mode. WLI, white-light imaging; ICI, intelligent chromo imaging; ICCE, intelligent chromo capsule endoscope; VoL, Variance of Laplacian. \*\*\*\* $P < 0.0001$ .

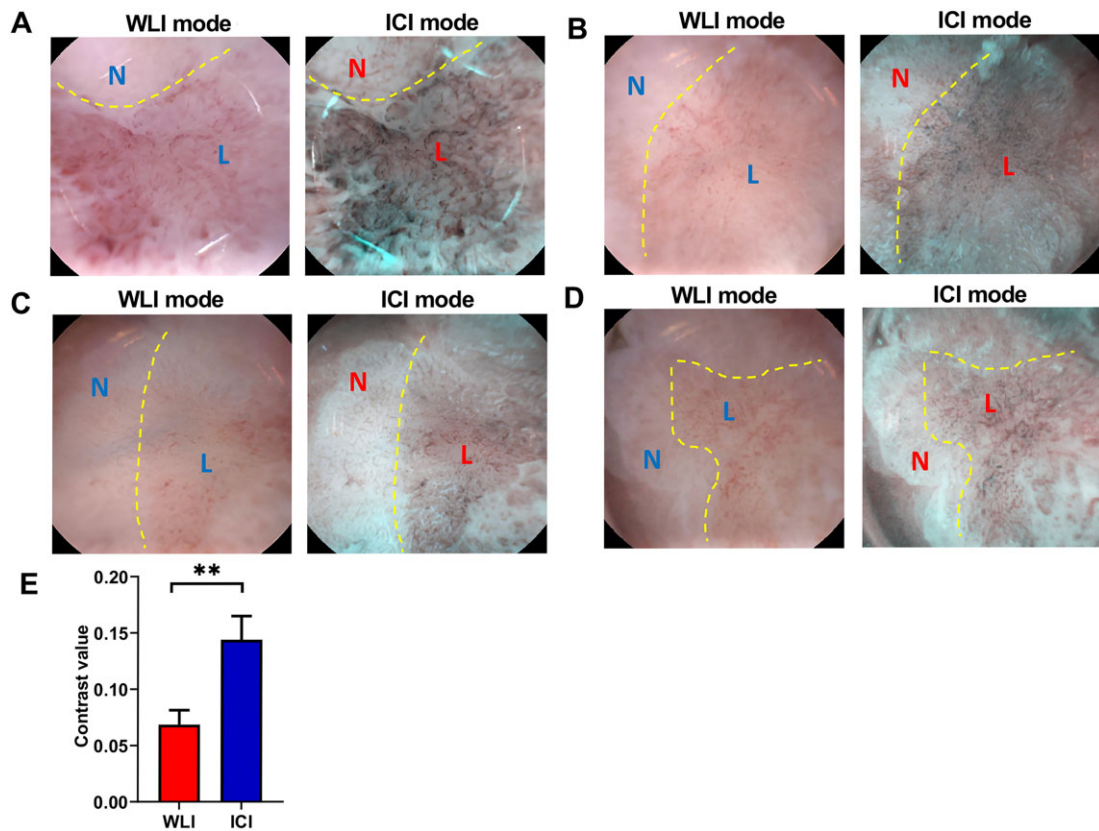


**Figure 6.** Comparison of WLI and ICI modes in the identification of non-tumor lesions and tumor lesions. (A)–(D) Representative images of non-lesion and lesion areas acquired in the WLI mode (left panel) and ICI mode (right) of the ICCE; (E) the contrast values were higher in the ICI mode than in the WLI mode. WLI, white-light imaging; ICI, intelligent chromo imaging; ICCE, intelligent chromo capsule endoscope; N, non-lesion area; L, lesion area. \*\* $P < 0.01$ .



**Table 2.** Contrast and VoL values and pixel intensities in images of gastrointestinal non-tumor lesions and tumor lesions acquired by WLI and ICI modes

Mode	Area	Red (R)	Green (G)	Blue (B)	Brightness ( $Y_N$ or $Y_L$ )	Contrast	P-value
WLI	N	153.077 ± 34.495	121.154 ± 28.629	119.615 ± 29.039	130.462 ± 30.082	0.069 ± 0.046	0.005
	L	157.923 ± 34.221	120.923 ± 29.960	116.540 ± 29.444	131.539 ± 30.886		
ICI	N	158.539 ± 23.599	168.231 ± 25.878	169.769 ± 25.940	165.462 ± 24.865	0.144 ± 0.076	
	L	164.385 ± 30.980	156.154 ± 31.026	157.077 ± 30.804	158.846 ± 30.838		

Data are presented as mean ± standard deviation. VoL, variance of Laplacian; WLI, white-light imaging; ICI, intelligent chromo imaging; N, non-tumor lesion area; L, tumor lesion area.

## Supplementary data

Supplementary data is available at *Gastroenterology Report* online.

## Authors' Contributions

R.L. designed and supervised the study including all data collection and analysis; H.S. and S.P. performed most of the investigation, including data collection and analysis, and wrote the manuscript; F.M. and T.Y. provided the technical support of the image analysis; S.T. performed some data analysis and interpretation. All authors read and approved the final version of the manuscript.

## Funding

This study was supported by the National Natural Science Foundation of China [grant numbers 82170571, 82100569, and 81974068] and the Natural Science Foundation of Hubei Province of China [grant number 2021CFB122].

## Acknowledgements

The authors wish to thank all study participants, researchers, clinicians, technicians, and administrative staff who contributed to this study.

## Conflict of Interest

The study was supported in part by Ankon company. Wuhan Union Hospital and Ankon company collaborated in this study. F.M. and T.Y. are research staff of Ankon Technologies Inc. All other authors have no conflicts of interest to disclose.

## References

- Bray F, Ferlay J, Soerjomataram I et al. Global cancer statistics 2018: GLOBOCAN estimates of incidence and mortality worldwide for 36 cancers in 185 countries. *CA Cancer J Clin* 2018;**68**: 394–424.
- Necula L, Matei L, Dragu D et al. Recent advances in gastric cancer early diagnosis. *World J Gastroenterol* 2019;**25**:2029–44.
- Mantese G. Gastrointestinal stromal tumor: epidemiology, diagnosis, and treatment. *Curr Opin Gastroenterol* 2019;**35**:555–9.
- Hayat M, Yang D, Draganov PV. Third-space endoscopy: the final frontier. *Gastroenterol Rep (Oxf)* 2023;**11**:goac077.
- Longcroft-Wheaton G, Bhandari P. Electronic chromoendoscopy. *Gastrointest Endosc* 2015;**82**:765.
- Lambert R, Kuznetsov K, Rey JF. Narrow-band imaging in digestive endoscopy. *ScientificWorldJournal* 2007;**7**:449–65.
- Kobayashi S, Yamada M, Takamaru H et al. Diagnostic yield of the Japan NBI Expert Team (JNET) classification for endoscopic diagnosis of superficial colorectal neoplasms in a large-scale clinical practice database. *United European Gastroenterol J* 2019;**7**:914–23.
- Misawa M, Kudo SE, Wada Y et al. Magnifying narrow-band imaging of surface patterns for diagnosing colorectal cancer. *Oncol Rep* 2013;**30**:350–6.
- Hu YY, Lian QW, Lin ZH et al. Diagnostic performance of magnifying narrow-band imaging for early gastric cancer: a meta-analysis. *World J Gastroenterol* 2015;**21**:7884–94.
- Griffin-Sobel JP. Gastrointestinal cancers: screening and early detection. *Semin Oncol Nurs* 2017;**33**:165–71.
- Ojidu H, Palmer H, Lewandowski J et al. Patient tolerance and acceptance of different colonic imaging modalities: an observational cohort study. *Eur J Gastroenterol Hepatol* 2018;**30**: 520–5.
- Thygesen MK, Baatrup G, Petersen C et al. Screening individuals' experiences of colonoscopy and colon capsule endoscopy: a mixed methods study. *Acta Oncol* 2019;**58**:S71–6.
- Ding Z, Wang W, Zhang K et al. Novel scheme for non-invasive gut bioinformation acquisition with a magnetically controlled sampling capsule endoscope. *Gut* 2021;**70**: 2297–306.
- Ching HL, Hale MF, Kurien M et al. Diagnostic yield of magnetically assisted capsule endoscopy versus gastroscopy in recurrent and refractory iron deficiency anemia. *Endoscopy* 2019;**51**:409–18.
- Liao Z, Hou X, Lin-Hu EQ et al. Accuracy of magnetically controlled capsule endoscopy, compared with conventional gastroscopy, in detection of gastric diseases. *Clin Gastroenterol Hepatol* 2016;**14**:1266–73.e1.
- Chetcuti Zammit S, Sidhu R. Capsule endoscopy: recent developments and future directions. *Expert Rev Gastroenterol Hepatol* 2021;**15**:127–37.
- Zhao AJ, Qian YY, Sun H et al. Screening for gastric cancer with magnetically controlled capsule gastroscopy in asymptomatic individuals. *Gastrointest Endosc* 2018;**88**:466–74.e461.
- Li Z, Liu J, Ji CR et al. Screening for upper gastrointestinal cancers with magnetically controlled capsule gastroscopy: a feasibility study. *Endoscopy* 2021;**53**:914–9.
- Kaneko K, Oono Y, Yano T et al. Effect of novel bright image enhanced endoscopy using blue laser imaging (BLI). *Endosc Int Open* 2014;**2**:E212–19.
- Kim S, Lee Y, Kim JY et al. Color-sensitive and spectrometer-free plasmonic sensor for biosensing applications. *Biosens Bioelectron* 2019;**126**:743–50.



21. Shahryari M, Meyer T, Warmuth C et al. Reduction of breathing artifacts in multifrequency magnetic resonance elastography of the abdomen. *Magn Reson Med* 2021;**85**:1962–73.
22. Santos D, Santana EEC, Junior P et al. Autofocus entropy repositioning method bioinspired in the magnetic field memory of the bees applied to pollination. *Sensors (Basel)* 2021;**21**:6198.
23. Yoshida N, Doyama H, Yano T et al. Early gastric cancer detection in high-risk patients: a multicentre randomised controlled trial on the effect of second-generation narrow band imaging. *Gut* 2021;**70**:67–75.
24. Liao Z, Zou W, Li ZS. Clinical application of magnetically controlled capsule gastroscopy in gastric disease diagnosis: recent advances. *Sci China Life Sci* 2018;**61**:1304–9.
25. Gu H, Zheng H, Cui X et al. Maneuverability and safety of a magnetic-controlled capsule endoscopy system to examine the human colon under real-time monitoring by colonoscopy: a pilot study (with video). *Gastrointest Endosc* 2017;**85**:438–43.
26. Keller J, Fibbe C, Volke F et al. Remote magnetic control of a wireless capsule endoscope in the esophagus is safe and feasible: results of a randomized, clinical trial in healthy volunteers. *Gastrointest Endosc* 2010;**72**:941–6.
27. Li Y, Wang X, Bao D et al. Optimal antiplatelet therapy for prevention of gastrointestinal injury evaluated by ANKON magnetically controlled capsule endoscopy: rationale and design of the OPT-PEACE trial. *Am Heart J* 2020;**228**:8–16.
28. Geropoulos G, Aquilina J, Kakos C et al. Magnetically controlled capsule endoscopy versus conventional gastroscopy: a systematic review and meta-analysis. *J Clin Gastroenterol* 2021;**55**:577–85.
29. Qian YY, Zhu SG, Hou X et al. Z: Preliminary study of magnetically controlled capsule gastroscopy for diagnosing superficial gastric neoplasia. *Dig Liver Dis* 2018;**50**:1041–6.
30. Vuik FER, Nieuwenburg SAV, Moen S et al. Colon capsule endoscopy in colorectal cancer screening: a systematic review. *Endoscopy* 2021;**53**:815–24.
31. Committee AT, Manfredi MA, Abu Dayyeh BK et al. Electronic chromoendoscopy. *Gastrointest Endosc* 2015;**81**:249–61.
32. Desai M, Viswanathan L, Gupta N et al. Impact of electronic chromoendoscopy on adenoma miss rates during colonoscopy: a systematic review and meta-analysis. *Dis Colon Rectum* 2019;**62**:1124–34.
33. Muto M, Minashi K, Yano T et al. Early detection of superficial squamous cell carcinoma in the head and neck region and esophagus by narrow band imaging: a multicenter randomized controlled trial. *JCO* 2010;**28**:1566–72.
34. Wani S, Rastogi A. Narrow-band imaging in the prediction of submucosal invasive colon cancer: how "NICE" is it? *Gastrointest Endosc* 2013;**78**:633–6.
35. Lan-Rong D, Yin-Yi W. A wireless narrowband imaging chip for capsule endoscope. *IEEE Trans Biomed Circuits Syst* 2010;**4**:462–8.
36. Yen CT, Lai ZW, Lin YT et al. Optical design with narrow-band imaging for a capsule endoscope. *J Healthc Eng* 2018;**2018**:5830759.